10th IMC
10th International Masonry Conference
G. Milani, A. Taliercio and S. Garrity (eds.)
Milan, Italy, July 9-11, 2018

NATURAL STONE MASONRY CHARACTERIZATION FOR THE SHAKING-TABLE TEST OF A SCALED BUILDING SPECIMEN

Ilaria Senaldi[1], Gabriele Guerrini[1], Simone Scherini[1], Simone Morganti[1], Guido Magenes[1,2], Katrin Beyer[3], and Andrea Penna[1,2]

[1] Department of Civil Engineering and Architecture, University of Pavia,
via Ferrata 3, 27100 Pavia, Italy.
{ilaria.senaldi,gabriele.guerrini,simone.morganti,guido.magenes,andrea.penna}@unipv.it,
simone.scherini01@universitadipavia.it,

[2] European Centre for Training and Research in Earthquake Engineering,
via Ferrata 1, 27100 Pavia, Italy.

[3] Civil Engineering Institute, École Polytechnique Fédérale de Lausanne,
Bâtiment CE 3316, Station 1, CH - 1015 Lausanne, Switzerland.
katrin.beyer@epfl.ch

Keywords: Natural stone masonry, Hydraulic lime mortar, Similitude relationships, Material characterization tests, Cyclic shear-compression tests.

Abstract. *This paper discusses the material characterization tests on stone masonry specimens, and the in-plane cyclic shear-compression tests on four half-scale unreinforced stone masonry piers, which complement a shaking-table test on a half-scale building aggregate prototype. Material characterization tests allowed defining a mortar composition suitable for satisfying the similitude relationships associated with the half-scale tests. Vertical and diagonal compression tests provided a complete description of the mechanical properties of masonry assemblies, while in-plane cyclic shear-compression tests allow determining the hysteretic behavior of masonry piers with different aspect ratios and axial compression levels. Strength and displacement capacities corresponding to the observed damage mechanisms and failure modes were also identified and associated with the specimens geometric and loading conditions. These activities are part of an experimental and numerical research project jointly carried by the University of Pavia, Italy, and the École Polytechnique Fédérale de Lausanne, Switzerland, which aims at assessing the seismic vulnerability of natural stone masonry building aggregates of the historical center of Basel, Switzerland.*

Peer-review under responsibility of the organizing committee of 10th ICM.

1 INTRODUCTION

In 1356 an earthquake with an estimated moment magnitude of 6.6 [1][2] devastated the city of Basel, Switzerland. Given the importance of the city in terms of population and economic activity concentration, the seismic vulnerability assessment of existing buildings and the mitigation of unacceptable risks with appropriate retrofit measures have become necessary tasks. Natural stone masonry building aggregates are of particular concern among other structures built before the first Swiss seismic regulations of 1970, because they constitute most of the historical center of Basel.

A fundamental characteristic of this type of construction is its strong heterogeneity, which results in difficult predictions of the masonry mechanical properties and of the structural behavior. For this reason, experimental information is essential at material, element, subassembly, and full building levels, in order to calibrate numerical models. Currently, only scarce data is available on the seismic performance of construction typologies specific to the Swiss practice [3], although extensive experimental campaigns have been performed on stone masonry buildings [4][12]. Furthermore, investigations on the response of building aggregates are limited to numerical simulations [13][14] or to case studies related to post-earthquake reconstruction projects [15].

These facts have prompted a joint research program between the University of Pavia, Italy, and the École Polytechnique Fédérale de Lausanne (EPFL), Switzerland, named "Seismic assessment of natural stone masonry buildings in Basel - A research and training project". Scopes of this program are advancing research on the seismic vulnerability and retrofit of stone masonry buildings, and training local engineers involved in practical applications of these concepts. As part of this project, a shake-table test [16][17] was performed on a half-scale model of a stone masonry building aggregate at the EUCENTRE laboratories in Pavia, Italy. Complementary tests on materials and components [18] were also conducted at EUCENTRE and at the Department of Civil Engineering and Architecture of the University of Pavia. This paper discusses the material characterization campaign and the in-plane cyclic shear-compression tests on four half-scale unreinforced stone masonry piers, including considerations of the similitude laws adopted for the half-scale building prototype for the dynamic test.

2 SIMILITUDE RELATIONSHIPS

Meeting similitude relationships is necessary whenever conducting a dynamic test on a scaled model, to obtain physically sound results. Despite the simplicity of scaling the horizontal accelerations imposed by the shake-table to the half-scale prototype, the effects of gravity acceleration could not be easily modified. Moreover, increasing the material density and thus the specimen weight would have exceeded the payload of the table. Therefore, a combination of scaling factors was chosen to avoid alteration of accelerations and mass densities [18], as listed in Table 1. Among other significant parameters, stresses, strengths and elastic moduli were scaled by the same factor $\lambda = 0.5$ applied to geometric lengths.

In order to achieve the masonry strength and stiffness reduction required by the similitude relationship, the mechanical properties of the mortar were modified [18]. The mortar was prepared starting from a hydraulic-lime plaster mix (a commercial product used for restorations of historic buildings), which belongs to the class CSII according to the European standard EN 1015-11 [19]. EPS beads, with volumetric proportions of 2 parts of EPS to 3 parts of commercial pre-mixed product (12 liters of EPS beads per 25-kg bag of product).

Parameter		Scaling factor
Geometric parameters	Length	λ
	Area	λ^2
	Volume	λ^3
	Moment of inertia	λ^4
Dynamic parameters	Displacement	λ
	Velocity	$\lambda^{1/2}$
	Acceleration	1
	Time	$\lambda^{1/2}$
	Period	$\lambda^{1/2}$
	Frequency	$\lambda^{-1/2}$
	Mass	λ^3
	Force	λ^3
Material parameters	Density	1
	Stress	λ
	Strain	1
	Young's modulus	λ
	Poisson's coefficient	1
	Shear modulus	λ
	Strength	λ
	Cohesion	λ

Table 1: Scaling factors.

3 MASONRY CHARACTERIZATION TESTS

3.1 Construction and geometry of the specimens

Historical buildings in the center of Basel typically consist of double-leaf stone masonry walls. The two leaves of such walls are usually weakly connected to each other and are separated by some filling material. In a large number of Basel's buildings through stones can be found only at corners and openings, while connection between the two leaves relies simply on the interlocking between irregular stones of adjacent leaves.

In order to reproduce the main characteristic of Basel's masonry in the half-scale prototype, the stones were roughly worked with a hammer and, in their final configuration, the blocks had irregular dimensions varying between 100 and 400 mm [16][17]. The stones were placed on mortar layers forming irregular horizontal courses. No through stones were provided across the wall thickness, except for the edge areas. The block irregularities resulted in variable space between the two leaves, which was filled with mortar, stone scraps, and pebbles. The thickness of the horizontal mortar layers varied between 5 and 20 mm depending on the stones shape and size. The density of the masonry resulted equal to 1980 kg/m^3.

Two walls were built aside during construction of the shake-table prototype, to be cut into several specimens for masonry characterization through vertical and diagonal compression tests [7]. The same materials and construction techniques adopted for the building prototype were used for the characterization walls. A nominal thickness of about 300 mm was selected, which is the average thickness of the walls of the shake-table prototype. Concrete tie-beams were provided top and bottom to the wall for vertical compression test specimens, to distribute the load during testing and to facilitate transportation. Tie-beams were not provided to the wall for diagonal compression test specimens, because they would have interfered with the test setup and execution.

Figure 1: Saw-cutting of a long wall to obtain specimens for vertical compression tests.

To avoid the confining effects of through stones necessary at the wall edges for construction, two long walls were built. Six individual wallettes were then obtained from each wall by saw-cutting it after 28 days of curing (Figure 1). A wall length of 400 mm was discarded at each edge: by doing this, the specimens were representative of a homogeneous masonry wall without through stones. Before saw-cutting, the walls were confined by vertical steel ties, intended to apply a low level of pre-compression and hence to reduce the risk of damage during cutting and transportation. The walls were cut using an electrical circular saw, consisting of a water-cooled steel-diamond disc, running on a metallic guide mounted on the wall itself.

Since standard dimensions of stone masonry specimens for vertical compression tests are not available, the prescriptions for brick masonry specified in the European standard EN 1052-1 [20] were adapted to stone masonry, replacing the size of the blocks with the average size of irregular stones. The dimensions of diagonal compression specimens were based on ASTM [21] and RILEM [22] standards, instead. Six rectangular wallettes with nominal dimensions of 1200 x 800 x 300 mm were obtained for vertical compression tests, labeled WV1 through WV6. Similarly, six square specimens with nominal dimensions of 1000 x 1000 x 300 mm were cut for diagonal compression tests, labeled WD1 through WD6. Three specimens of each series, labeled PL, had plaster on one face, consisting of a 10-mm-thick hydraulic-lime plaster layer and a 5-mm-thick non-hydraulic-lime plaster finish.

3.2 Vertical compression tests

Six rectangular specimens (Figure 2) were subjected to vertical compression tests [7][20]. The testing apparatus consisted of a force-controlled universal testing machine and displacement transducers. The applied axial compression was centered on the wall and distributed as uniformly as possible on the cross-section by spreader beams and tie-beams. Loading and unloading cycles of increasing amplitude were applied to the specimens, in increments of 24.5 kN. For each cycle, the maximum load was held constant for about 60 seconds before unloading, to stabilize the stress state in the specimen.

Longitudinal and transverse deformations were measured by eight 25-mm-stroke potentiometers, located as shown in Figure 2. Four transducers (two on each face) were used to obtain vertical longitudinal strains, two (one on each face) to measure horizontal transverse strains in the wall plane, and two (one on each side) to determine horizontal transverse strains over the wall thickness [18]. The nominal length between the mounting rods of the transducers was adjusted case by case to ensure they were installed only in stones of sufficient size, avoiding mortar joints; for this reason, the actual lengths were measured for each specimen.

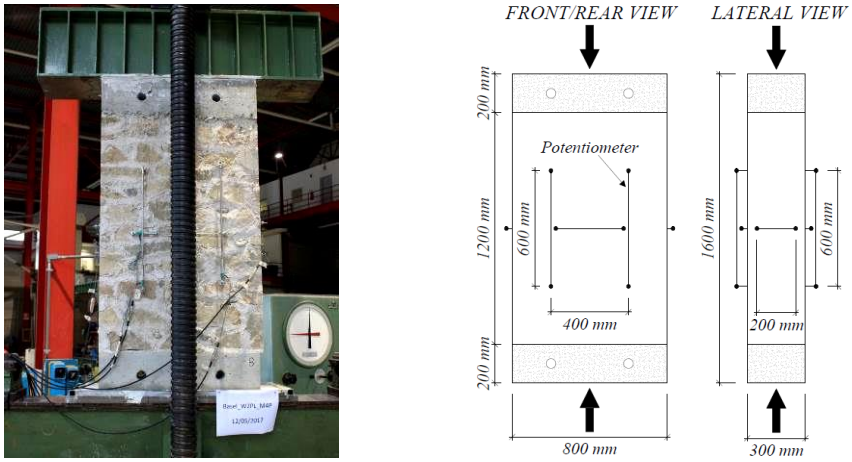

(a) (b)

Figure 2: Vertical compression test: (a) test setup, and (b) specimen dimensions.

The masonry vertical compressive stress was computed assuming that boundary conditions (concrete tie-beams) did not have any influence on the state of stress within the middle half of the panel, where the instrumentation was installed. The applied force was divided by the nominal cross-section area A_n = 2.4 x 10^5 mm^2, that is the product of the specimen thickness (300 mm) times the wallette length (800 mm). The compressive strength f_c was evaluated by testing the specimen up to failure, and taking the maximum applied force [18].

The masonry elastic constants were calculated with the additional assumptions that masonry behaves as a homogeneous, isotropic, and linearly elastic material at low stress levels, and that deformations only depend on the level of vertical compression. In particular, Young's modulus E was evaluated as the slope of the secant line on the longitudinal stress-strain plane, between 10% and 33% of the measured compressive strength. Poisson's ratio ν was estimated as the ratio of the differential average transverse strain to the differential average longitudinal strain, also between at 10% and 33% of the measured compressive strength. Finally, the shear modulus G was calculated using its linear-elasticity relationship with E and ν [18].

The results of the vertical compression tests are shown in Table 2. Figure 3a presents the response of specimen WV2PL in terms of vertical compressive stress versus vertical compressive and horizontal tensile strains. Figure 3b shows a zoom of the vertical compressive stress-strain response with a straight line through the points at 10% and 33 % of the compressive strength: the slope of this line is the Young's modulus E. A plateau was recorded in the stress-strain response when the applied force was held constant, especially at higher stresses: this is indicative of a viscous behavior. Some tests were previously conducted varying the loading rate, with no significant effects on compressive strength or elastic parameters.

Specimen	f_c [MPa]	E [MPa]	υ [-]	G [MPa]
WV1PL	1.32	3343	0.12	1497
WV2PL	1.34	4214	0.03	2045
WV3PL	1.24	3532	0.23	1438
WV4	1.29	3218	0.21	1332
WV5	1.29	2984	0.08	1384
WV6	1.29	3481	0.20	1449

Table 2: Results of the vertical compression tests.

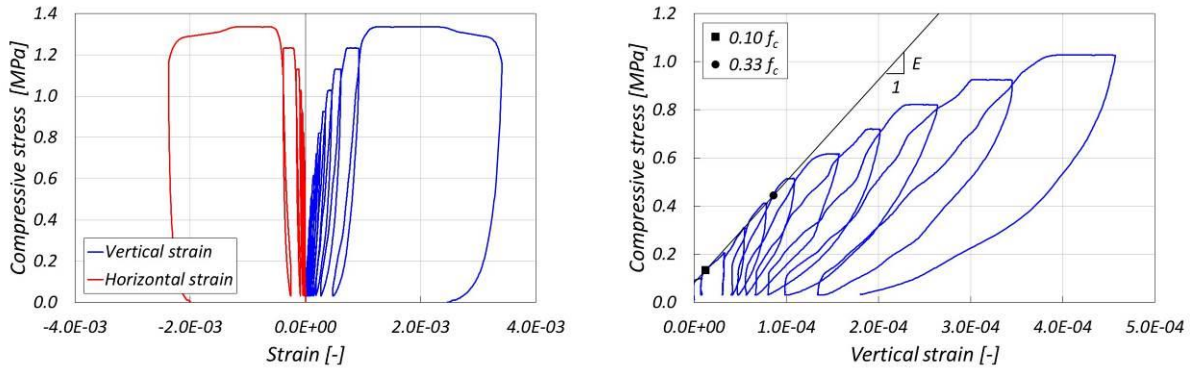

(a) (b)

Figure 3: Response of specimen WV2PL: (a) vertical compressive stress versus vertical and horizontal strains, and (b) determination of E from low-amplitude cycles.

3.3 Diagonal compression tests

Six square specimens (Figure 4) were subjected to diagonal compression tests [7][21][22]. The testing apparatus consisted of a force-controlled universal testing machine and displacement transducers. The compressive force was applied along a diagonal of the square masonry panel, leaving the other diagonal unloaded. Loading and unloading cycles of increasing amplitude were applied to the specimens, in increments of 15.7 kN. For each cycle, the maximum load was held constant for about 20 seconds before unloading, to stabilize the stress state in the specimen.

Deformations were measured along the two diagonals with four 25-mm-stroke potentiometers, located on both faces as shown in Figure 4. Shear strains were derived from the diagonal deformations [18]. The nominal length between the mounting rods of the transducers was adjusted case by case to ensure they were installed only in stones of sufficient size, avoiding mortar joints; for this reason, the actual lengths were measured for each specimen.

The ASTM [21] and RILEM [22] standards interpret the results assuming a pure-shear stress state at the center of the panel. The corresponding Mohr circle (Figure 5a) is centered on the origin of the σ-τ plane, resulting in principal tensile and compressive stresses, σ_t and $|\sigma_c|$, and shear stress τ all equal to the radius of the circle. The stresses in Figure 5 are normalized by P/A_n, where P is the applied compression force and A_n = 3 x 10^5 mm^2 is the

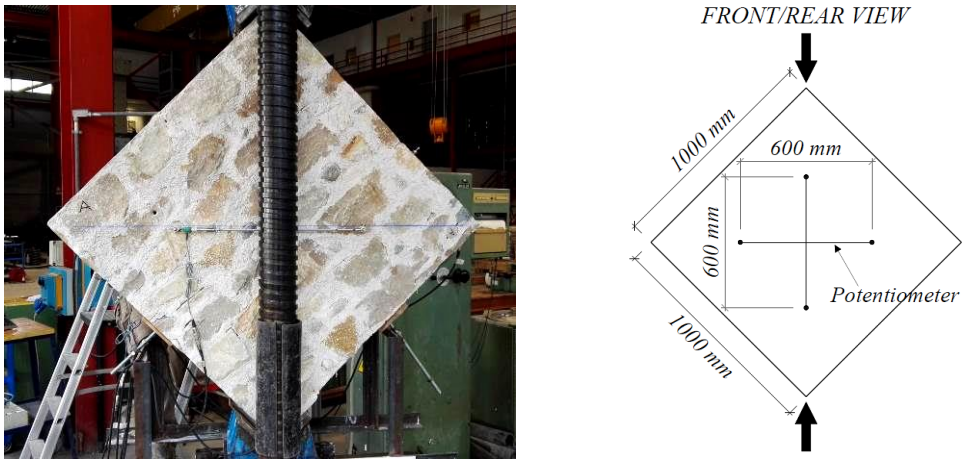

(a) (b)

Figure 4: Diagonal compression test: (a) test setup, and (b) specimen dimensions.

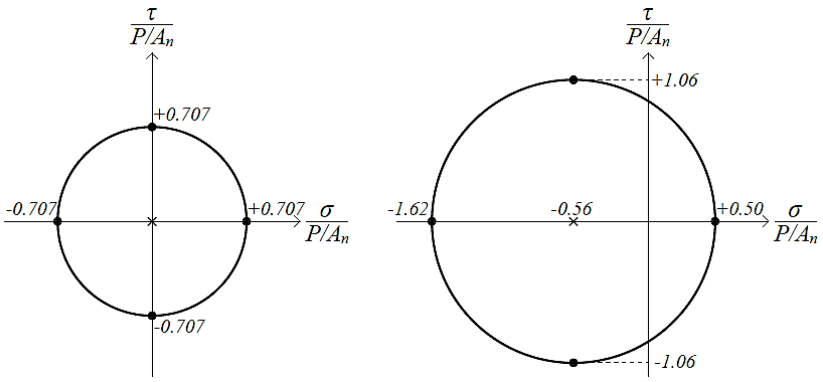

Figure 5: Mohr circles of the diagonal compression test: (a) standard interpretation, and (b) refined interpretation. Tension positive.

nominal area subjected to uniform shear stress, that is the product of the specimen thickness (300 mm) times the side length (1000 mm). The maximum shear stress τ_{max} was evaluated by testing the specimen up to failure, and taking the maximum applied force. Under the hypothesis of homogeneous, isotropic, and linearly elastic material subjected to a pure-shear stress state, the shear modulus G was evaluated as the slope of the secant line on the shear stress-strain plane, between 10% and 33% of the maximum shear stress [18].

While this approach can be sufficiently accurate for estimating the shear modulus, from the average shear strain and stress in the panel area instrumented with potentiometers, the actual distribution of shear stresses is far from uniform and the panel is not subject to pure shear. This problem has been studied by several authors, following both analytical and numerical procedures [23][24], who suggested more correct formulations to evaluate the principal stresses at the center of the panel (Figure 5b). In particular, the refined principal tensile stress f_t compares to the standard maximum shear stress τ_{max} with a ratio of 0.5 to 0.707. It is believed that this second interpretation is more appropriate in predicting the masonry tensile strength [7], because cracks are expected to develop when the principal tensile stress equals the strength at the center of the panel. The masonry tensile strength was evaluated by testing the specimen up to failure, taking the principal tensile strength corresponding the maximum force reached during the test [18].

The results of the diagonal compression tests are shown in Table 3. Figure 6a presents the response of specimen WD2PL in terms of shear stress and strain. Figure 6b shows a zoom of the shear stress-strain response with a straight line through the points at 10% and 33 % of the maximum shear stress: the slope of this line is the shear modulus G.

Specimen	f_t [MPa]	τ_{max} [MPa]	G [MPa]
WD1PL	0.15	0.22	1789
WD2PL	0.19	0.27	1446
WD3PL	0.16	0.23	750
WD4	0.16	0.23	1790
WD5	0.16	0.23	1603
WD6	0.17	0.24	4010

Table 3: Results of the diagonal compression tests.

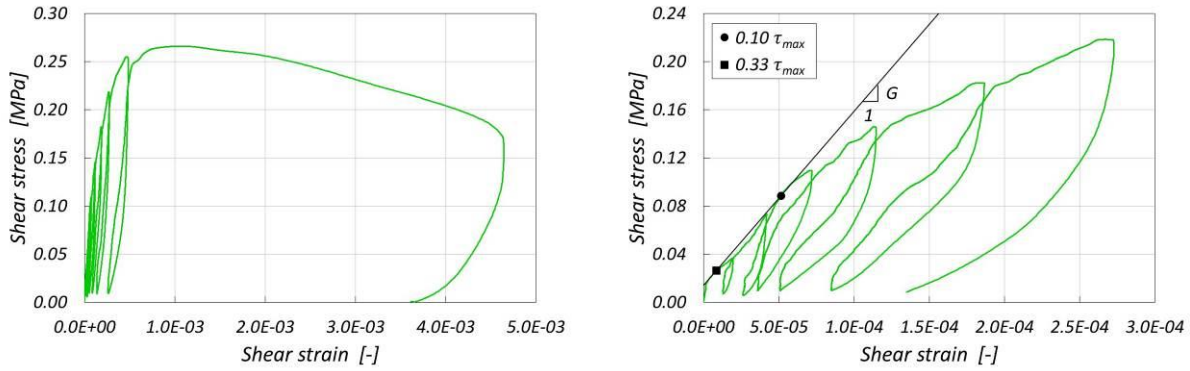

(a) (b)

Figure 6: Response of specimen WD2PL: (a) shear stress-strain relationship, and (b) determination of *G* low-amplitude cycles.

3.4 Summary of masonry mechanical properties

The mean values and the dispersion of the masonry mechanical properties evaluated through vertical and diagonal compression test are summarized in Table 4. The masonry compressive strength of 1.3 MPa obtained for the half-scale prototype is compatible with the similitude relationships governing the dynamic test. In fact, full-scale material tests on masonry representative of Basel's historical buildings conducted at EPFL resulted in compressive strength of about 2.5 MPa.

Little dispersion was found for the compressive and tensile strengths, calculated from the recorded forces, with coefficient of variations smaller than 10%. On the other hand, potentiometers readings were very sensitive to measurement errors especially in the direction perpendicular to the applied load, given the small amplitude of the transverse displacements during the initial loading cycles. This caused large scatter on the Poisson's coefficient determined from the vertical compression tests and on the shear modulus derived from the diagonal compression tests, with coefficients of variation of about 60%. Obtaining the shear modulus indirectly from vertical compression tests rather than directly from diagonal compression tests resulted in smaller dispersion. In fact, Young's modulus was characterized by a coefficient of variation of only 12% and the scatter of Poisson's ratio at the denominator $2(1+\nu)$ had little influence being $\nu << 1$.

A discrepancy of the order of 25% was observed between the shear moduli obtained from the two test series. The main reason for this difference can be attributed to the assumption of homogeneity and isotropy of the material, which is intrinsically violated by the texture of stone masonry.

	f_c [MPa]	f_t [MPa]	E [MPa]	υ [-]	$G^{(1)}$ [MPa]	$G^{(2)}$ [MPa]
Mean	1.30	0.17	3462	0.14	1524	1898
St. dev.	0.03	0.012	418	0.08	261	1104
C.o.v.	2.6%	7.3%	12%	56%	17%	58%

(1) From vertical compression tests
(2) From diagonal compression tests

Table 4: Summary results of mechanical characterization tests on masonry wallettes.

4 IN-PLANE CYCLIC SHEAR-COMPRESSION TESTS ON PIERS

4.1 Construction and geometry of the specimens

In-plane cyclic shear-compression tests allow determining the behavior of masonry piers subjected to horizontal cyclic forces in their plane. In particular, information about lateral strength, stiffness, displacement/deformation capacity, and hysteretic energy dissipation can be obtained. Several parameters affect the in-plane response of piers. Among others, material characteristics, element geometry, restraint conditions, and axial compression level are the most significant ones [8][25].

Four masonry piers were built during construction of the shake-table prototype for in-plane cyclic shear-compression tests, using the same materials and construction techniques adopted for the half-scale building prototype. A nominal thickness of about 300 mm was selected, which is the average thickness of the walls of the shake-table prototype. In order to better represent piers of the building prototype, double-bending conditions were imposed to the specimens, and two aspect ratios (i.e. ratio of pier height h to length ℓ) were selected: $h/\ell = 1.26$ for two squat piers CT02 and CT01 (Figure 7a) and $h/\ell = 3.0$ for two slender piers CS01 and CS02 (Figure 7b). For each aspect ratio, two axial compression levels (i.e. ratio of uniform normal stress $\sigma_{0,bot}$ at the base to masonry compressive strength f_c) at the pier base were targeted: 0.2 and 0.3 for CT02 and CT01, and 0.3 and 0.45 for CS01 and CS02, respectively. One face of each pier was plastered similarly to the material characterization wallettes.

4.2 Test setup and protocol

The experimental setup for in-plane cyclic tests took advantage of the three-dimensional strong-walls/strong-floor configuration of the EUCENTRE laboratory [8][26]. Fundamental parts of this system were three servo-hydraulic actuators, with a maximum force capacity of 250 kN each and a stroke of 0.76 m. Two actuators applied an axial load to the specimen, while the third one imposed horizontal displacements to the top of the piers in the North-South direction (Figure 8). Since a double-bending configuration was chosen for the tests, vertical rotation of the pier top was prevented by the implementation of a hybrid control of the vertical actuators: they were forced to apply a constant total axial load and to maintain the same vertical displacement. Out-of-plane displacements of the pier top were prevented by specific restraints, allowing longitudinal translation only.

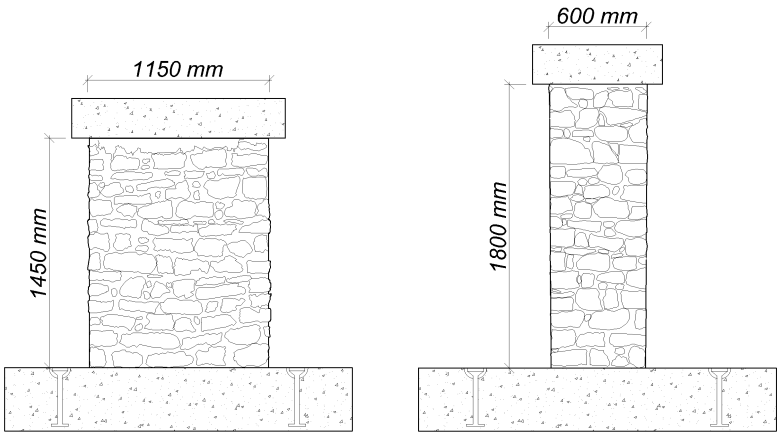

Figure 7: Cyclic shear-compression test specimens: (a) dimensions of squat piers CT01 and CT02; (b) dimensions of slender piers CS01 and CS02.

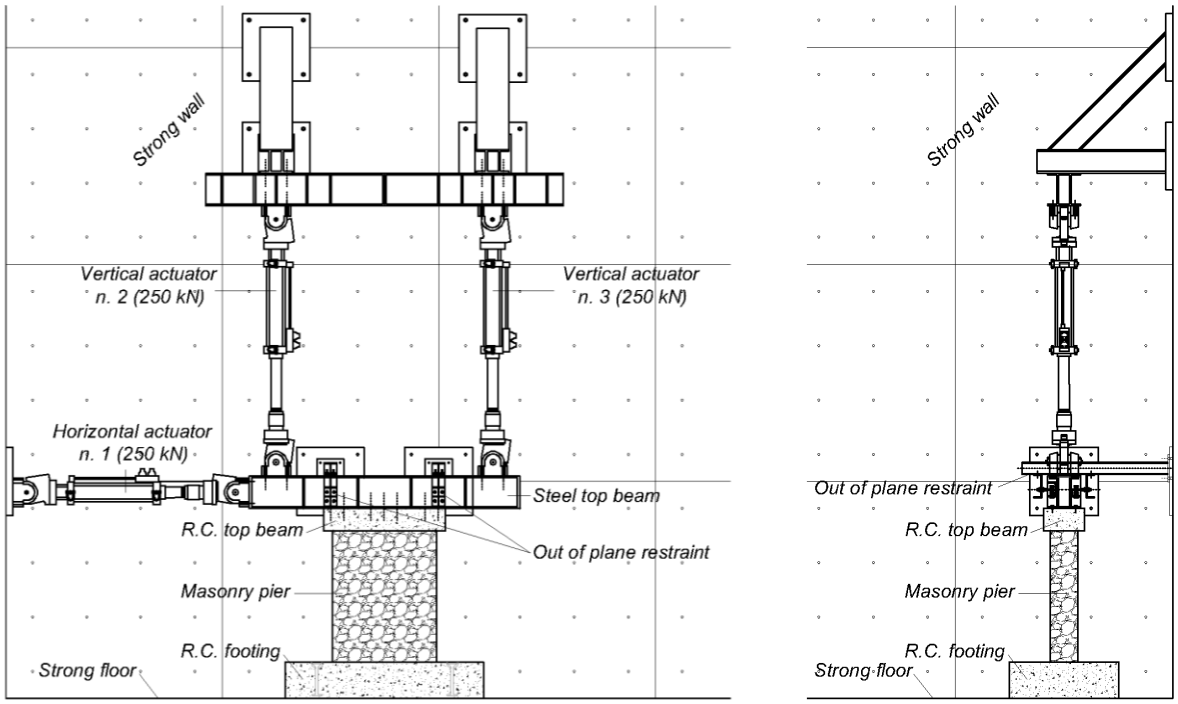

Figure 8: Test setup: (a) front view, and (b) side view.

The specimens were densely instrumented with 28 displacement transducers, mounted on the non-plastered West face and on the North and South sides, to derive relative and absolute displacements and local deformations. A three-dimensional optical motion-capture system was instead employed on the plastered East face: passive retro-reflective spherical markers were glued to the pier surface and were monitored by fixed cameras recording their coordinates as they varied during the tests.

The first loading phase consisted of gradually applying the vertical load to the specimen in force control, until the target value was reached. Then, keeping the total vertical load constant, a rotation was imposed to the steel beam to compensate for the eccentricity of the horizontal actuator weight. Once equilibrium was established, with the vertical load centered on the masonry pier, the rotation of the steel beam was locked in for all subsequent testing phases.

In the following phase, the horizontal actuator was set in force control, and the pier was subjected to three push-and-pull cycles with force amplitude equal to 1/4 of its analytical shear strength and loading rate of 0.5 kN/s. This first sequence of loading was labeled 1F. The two following sequences of three cycles each, called 2F and 3F, were conducted either in force or displacement control, depending on the extent of nonlinearity observed on the recorded force-displacement response. Sequences 2F and 3F had amplitudes multiple of the lateral force or displacement reached in 1F, and loading rates of 0.5 kN/s or 0.025 mm/s.

Finally, once a drift ratio $\theta = \delta/h$ (i.e. lateral top displacement δ normalized by the pier height h) of 0.05% was reached, a protocol consisting of displacement-controlled "D" sequences of increasing amplitude (Table 5) was followed. If the drift to be applied at sequence 1D was less than (or approximately equal to) those obtained for cycles 2F or 3F, those "F" cycles were skipped. The test was stopped if the specimen presented a potentially dangerous damage or a significant drop of lateral strength.

Sequence	CT02 and CT01		CS01 and CS02	
	Load rate [mm/s]	Drift ratio [%]	Load rate [mm/s]	Drift ratio [%]
1D	0.029	0.05	0.036	0.05
2D	0.035	0.075	0.043	0.075
3D	0.039	0.10	0.048	0.10
4D	0.044	0.15	0.054	0.15
5D	0.046	0.20	0.058	0.20
6D	0.058	0.25	0.072	0.25
7D	0.070	0.30	0.086	0.30
8D	0.093	0.40	0.115	0.40
9D	0.116	0.50	0.144	0.50
10D	0.139	0.60	0.173	0.60
11D	0.162	0.70	0.202	0.70
12D	0.186	0.80	0.230	0.80
13D	0.232	1.00	0.288	1.00
14D	0.290	1.25	0.360	1.25
15D	0.290	1.50	0.432	1.50
16D	0.290	1.75	0.576	2.00
17D	0.290	2.00	0.846	3.00
18D	0.348	3.00	1.152	4.00
19D	-	-	1.440	5.00

Table 5: Summary of the test sequences.

4.3 Main test outcomes

Flexural rocking behavior dominated specimens CT02 (h/ℓ = 1.26 and $\sigma_{0,bot}/f_c$ = 0.2) and CS01 (h/ℓ = 3.0 and $\sigma_{0,bot}/f_c$ = 0.3). The rocking mechanism fully activated on pier CT02 at θ = 0.25%, with horizontal cracks extending for the entire length at the base and below the top stone layer; mortar crushing was observed close to the top corners at θ = 0.8%, while two stones fell from the upper corners at θ = 1.75% and θ = 2%. Similarly, specimen CS01 fully developed its rocking mechanism after reaching θ = 0.7%; mortar started crushing along the top horizontal crack at θ = 2%, while at θ = 4% one stone cracked and one was expelled at the upper corners. These two specimens were able to sustain maximum drift ratios θ_{max} of 3% and 5%, respectively, before showing extensive toe crushing (Figure 9).

CT02 h/ℓ = 1.26 $\sigma_{0,bot}/f_c$ = 0.20 θ_{max} = 3%

CT01 h/ℓ = 1.26 $\sigma_{0,bot}/f_c$ = 0.30 θ_{max} = 1.75%

CS01 h/ℓ = 3.00 $\sigma_{0,bot}/f_c$ = 0.30 θ_{max} = 5%

CS02 h/ℓ = 3.00 $\sigma_{0,bot}/f_c$ = 0.45 θ_{max} = 3%

Figure 9: Damage conditions the four specimens at the end of testing.

Hybrid mechanisms were observed on the more heavily loaded piers CT01 (h/ℓ = 1.26 and $\sigma_{0,bot}/f_c$ = 0.3) and CS02 (h/ℓ = 3.0 and $\sigma_{0,bot}/f_c$ = 0.45). A flexural rocking mechanism fully activated on specimen CT01 at θ = 0.20%, with horizontal cracks extending for the entire length at the base and below the top stone course. During the θ = 0.25% sequence, however, diagonal and vertical cracks started forming, and from the θ = 0.5% sequence, increasing bulging was recorded: diagonal strut failure triggered a shear failure accompanied by toe crushing at the base (Figure 9), with maximum drift ratio θ_{max} = 1.75%. Similarly, slender pier CS02 fully developed its rocking mechanism at θ = 0.5%, with mortar crushing close to the top corners beginning at θ = 0.7%. From the θ = 1.5% sequence, however, vertical and diagonal cracks started forming and progressive bulging was recorded: at the end of the test (θ_{max} = 3%), diagonal strut failure and toe crushing were simultaneously observed (Figure 9), with stone expulsion at one bottom corner.

The hysteretic responses of the four specimens are depicted on Figure 10, in terms of drift ratio θ and base-shear coefficient $BSC = V/N_{bot}$ (i.e. shear force V normalized by the bottom axial compression N_{bot}). Backbone curves are also shown on the figure. The degrading cycles recorded for pier CT01 denote a shear-dominated behavior, as a shear mechanism was triggered by failure of the diagonal struts. Instead, the hysteretic responses of the other three specimens confirmed their flexure-dominated behavior, despite pier CT02 showed non-negligible sliding over the top and bottom horizontal rocking cracks and pier CS02 ultimately failed because of diagonal strut crushing.

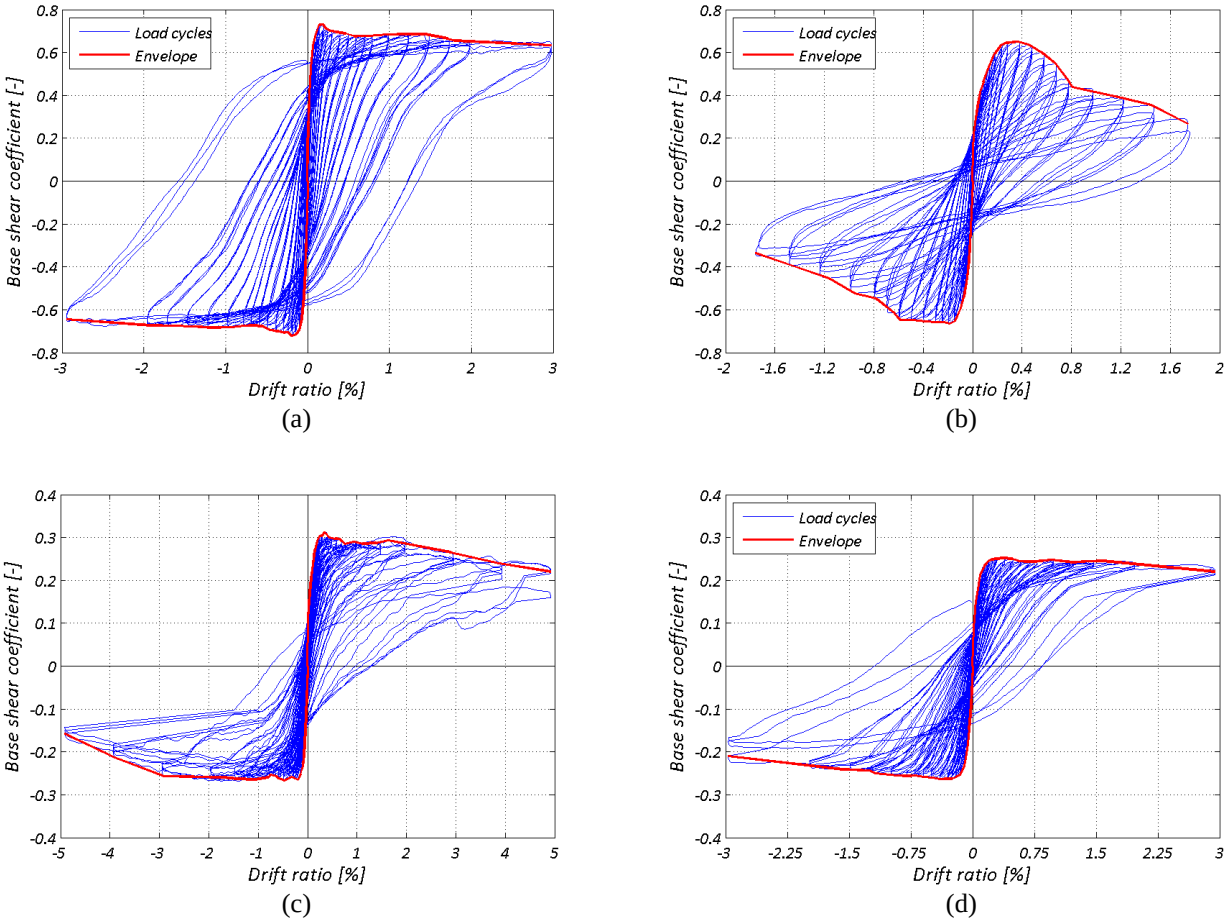

Figure 10: Hysteretic responses and backbone curves: (a) CT02, (b) CT01, (c) CS01, (d) CS02.

4.4 Summary of the results

Table 6 summarizes the cyclic shear-compression test results. The average values from the positive and negative force-displacement envelopes are reported for each specimen. In particular, one can observe that, for given aspect ratio, increasing the axial compression results in higher lateral strength V_{max}; however, the base-shear coefficient BSC_{max} reduces when the axial compression increases. Similarly, the ultimate drift-ratio capacity θ_u at residual lateral strength equal to 80% of the peak one decreases as the axial compression level increases.

Slender piers CS01 and CS02 reached larger drift ratios θ_u compared to squat specimens CT02 and CT01, due to higher elastic flexibility and prevailing rocking response. The base-shear coefficient capacities BSC_{max}, instead, were significantly lower for the slender piers than for the squat ones.

Plaster started cracking at drift ratios of about 0.05%, and started spalling off at about 0.3% in all specimens. Larger areas were interested by plaster spalling under higher axial compression levels.

Parameter	Units	CT02	CT01	CS01	CS02
h/ℓ	-	1.26	1.26	3.00	3.00
$\sigma_{0,bot}/f_c$	-	0.20	0.30	0.30	0.45
N_{bot}	kN	90	135	67	105
V_{max}	kN	65	89	19	27
BSC_{max}	-	0.725	0.657	0.289	0.258
θ_u	%	2.95	0.798	3.69	2.94

Table 6: Summary results of in-plane cyclic shear-compression tests.

5 CONCLUSIONS

This paper described the material and component characterization campaign on natural stone masonry employed for the half-scale dynamic test of a building prototype representative of the historical center of Basel, Switzerland. A mortar obtained from a commercial hydraulic-lime mix, with addition of EPS beads, was used to reduce the stiffness and strength of the material, according to the similitude relationships adopted for the scaled dynamic test. An experimental investigation conducted at EPFL on specimen reproducing historical stone-masonry, provided mean masonry compressive strength of about 2.5 MPa. The mean compressive strength of 1.3 MPa obtained for the half-scale prototype is then compatible with the similitude laws governing the dynamic test.

Little dispersion was found for the masonry compressive and tensile strengths and for its Young's modulus, with coefficient of variations of the order of 10% or less. Large scatter was observed on Poisson's coefficient from vertical compression tests and on the shear modulus from diagonal compression tests, due to the precision of potentiometers measuring very small transverse displacements: coefficients of variation of about 60% were found for these parameters. Obtaining the shear modulus indirectly from vertical compression tests rather than directly from diagonal compression tests resulted in smaller dispersion. A discrepancy of the order of 25% was observed between the shear moduli obtained from the two test series. The main reason for this difference can be attributed to the assumption of homogeneity and isotropy of the material, which is intrinsically violated by the texture of stone masonry.

The behavior of masonry piers was dominated by flexural rocking under lower axial compression for both aspect ratios, even though the squatter pier exhibited also sliding along the top and bottom horizontal rocking cracks. The heavily loaded squat pier displayed a hybrid

failure mechanism, beginning with a flexural rocking mode and transitioning towards a shear failure triggered by diagonal strut crushing; this was confirmed by its degrading cyclic force-displacement response. A hybrid response was recorded for the highly compressed slender specimen as well: after the initial development of a rocking mechanism, this pier ultimately failed because of diagonal strut crushing. Plaster started cracking at drift ratios of about 0.05%, and started spalling off at about 0.3% in all specimens; larger areas were interested by plaster spalling under higher axial compression levels.

The material properties and the pier hysteretic behaviors obtained from these experimental campaigns will be used for the calibration of numerical models. These will have the objective of reproducing the response of the shake-table prototype, and then of predicting the performance of other stone masonry buildings with similar characteristics.

ACKNOWLEDMENTS

This work is part of the research project "Seismic assessment of natural stone masonry buildings in Basel - A research and training project", jointly carried by the École Polytechnique Fédérale de Lausanne and the University of Pavia, partially funded by the Swiss Federal Office for the Environment and the Canton Basel-City.

The authors would like to thank Mapei S.p.a. for its support to the project. The help provided during the tests by P. Comini, Dr. F. Graziotti, L. Grottoli, M. Mandirola, and S, Pellegrini is gratefully acknowledged.

REFERENCES

[1] D. Fäh, M. Gisler, B. Jaggi, P. Kästli, T. Lutz, V. Masciadri, C. Matt, D. Mayer-Rosa, D. Rippmann, G. Schwartz-Zanetti, J. Tauber, T. Wenk, The 1356 Basel earthquake: an interdisciplinary revision. *Geophysical Journal International*, **178**(1), 351-374, 2009.

[2] T. Wenk, D. Fäh, Seismic Microzonation of the Basel Area. *Proc. of the 15th World Conference on Earthquake Engineering*, September 24-28, Lisbon, Portugal, 2012

[3] C. Michel, P. Lestuzzi, M. Oropeza, E. Lattion, *Seismic Vulnerability of Swiss Masonry Buildings: Findings and Issues*. Research report, École Polytechnique Fédérale de Lausanne, Switzerland, 2008.

[4] M. Tomaževic, P. Weiss, T. Velechovsky, The influence of rigidity of floors on the seismic behaviour of old stone-masonry buildings. *European Earthquake Engineering*, **3,** 28-41, 1991

[5] D. Benedetti, P. Carydis, P. Pezzoli, Shaking table test on 24 masonry buildings. *Earthquake Engineering and Structural Dynamics*, **27**(1), 67-90, 1998.

[6] N. Mazzon, C.M. Chavez, M.R. Valluzzi, F. Casarin, C. Modena, Shaking table tests on multi-leaf stone masonry structures: Analysis of stiffness decay. *Advanced Materials Research*, **133**, 647-652, 2010.

[7] G. Magenes, A. Penna, A. Galasco, M. Rota, Experimental characterisation of stone masonry mechanical properties. *Proc. of the 8th International Masonry Conference*, July 4-7, Dresden, Germany, 2010, 247-256.

[8] G. Magenes, A. Penna, A. Galasco, M. Da Parè, In-plane cyclic shear tests of undressed double-leaf stone masonry panels. *Proc. of the 8th International Masonry Conference*, July 4-7, Dresden, Germany,2010.

[9] G. Magenes, A. Penna, A. Galasco, A full-scale shaking table test on a two-storey stone masonry building. *Proc. of the 14th European Conference on Earthquake Engineering*, Aug. 30-Sept. 3, Ohrid, Rep. of Macedonia, 2010.

[10] G. Magenes, A. Penna, I.E. Senaldi, M. Rota, A. Galasco, Shaking table test of a strengthened full-scale stone masonry building with flexible diaphragms. *International Journal of Architectural Heritage*, **8**(3), 349-375, 2014.

[11] I. Senaldi, G. Magenes, A. Penna, A. Galasco, M. Rota, The effect of stiffened floor and roof diaphragms on the experimental seismic response of a full-scale unreinforced stone masonry building. *Journal of Earthquake Engineering*, **18**(3), 407-443, 2014.

[12] E. Vintzileou, C. Mouzakis, C.E. Adami, L. Karapitta, Seismic behavior of three-leaf stone masonry buildings before and after interventions: Shaking table tests on a two-storey masonry model. *Bulletin of Earthquake Engineering*, **13**(10), 3107-3133, 2015.

[13] I. Senaldi, G. Magenes, A. Penna, Numerical investigations on the seismic response of masonry building aggregates. *Advanced Materials Research*, **133,** 715-720, 2010.

[14] A. Formisano, Theoretical and numerical seismic analysis of masonry building aggregates: case studies in San Pio Delle Camere (L'Aquila, Italy). *Journal of Earthquake Engineering*, **21**(2), 227-245, 2017.

[15] F. Da Porto, M. Munari, A. Prota, C. Modena, Analysis and repair of clustered buildings: Case study of a block in the historic city centre of L'Aquila (Central Italy). *Construction and Building Materials*, **38,** 1221-1237, 2013.

[16] I. Senaldi, G. Guerrini, F. Graziotti, M. Caruso, F. Di Santo, P. Comini, G. Magenes, K. Beyer, A. Penna, Shaking-table test of a half-scaled natural stone masonry building aggregate with flexible diaphragms. *Proc. of the 17th ANIDIS Conference "L'Ingegneria Sismica in Italia"*, September 17-21, Pistoia, Italy, 2017.

[17] G. Guerrini, I. Senaldi, F. Di Santo, U. Tomassetti, F. Graziotti, G. Magenes, K. Beyer, A. Penna, Experimental seismic response of a half scale natural stone masonry building prototype. *Proc. of the 10th International Masonry Conference*, July 9-11, Milan, Italy, 2018.

[18] G. Guerrini, I. Senaldi, S. Scherini, S. Morganti, G. Magenes, K. Beyer, A. Penna, Material characterization for the shaking-table test of the scaled prototype of a stone masonry building aggregate. *Proc. of the 17th ANIDIS Conference "L'Ingegneria Sismica in Italia"*, September 17-21, Pistoia, Italy, 2017.

[19] EN 1015-11:1999/A1:2006: Methods of test for mortar for masonry - Part 11: Determination of flexural and compressive strength of hardened mortar. CEN European Committee for Standardization: Brussels, Belgium, 2006.

[20] EN 1052-1:1998: Methods of test for masonry - Part 1: Determination of compressive strength. CEN European Committee for Standardization: Brussels, Belgium, 1998.

[21] ASTM E519-15: Standard Test Method for Diagonal Tension (Shear) in Masonry Assemblages. ASTM International: West Conshohocken, PA, USA, 2015.

[22] RILEM LUM-B6: Diagonal Tensile Strength Tests of Small Wall Specimens. RILEM Recommendation: E. & F.N. Spon Ltd., London, UK, 1991.

[23] M.M. Frocht, Recent advances in photoelasticity and an investigation of the stress distribution in square blocks subjected to diagonal compression. *Transactions of the American Society of Mechanical Engineers*, *Applied Mechanics Division*, **53**(15), 135-153, 1931.

[24] A. Brignola, S. Frumento, S. Lagomarsino, S. Podestà, Identification of shear parameters of masonry panels through the in-situ diagonal compression test, *International Journal of Architectural Heritage*, **3**(1), 52-73, 2009.

[25] G. Magenes, G.M. Calvi, In-plane seismic response of brick masonry walls. *Earthquake Engineering and Structural Dynamics*, **26**(11), 1091-1112, 1997.

[26] G. Magenes, P. Morandi, A. Penna, *Test results on the behaviour of masonry under static cyclic in plane lateral loads.* Research report RS-01/08, Department of Structural Mechanics, University of Pavia, Italy, 2008.